Computers and Electronics in Agriculture 135 (2017) 233–241

Contents lists available at ScienceDirect

Computers and Electronics in Agriculture

journal homepage: www.elsevier.com/locate/compag

Original papers

Near-infrared imaging to quantify the feeding behavior of fish in aquaculture

Chao Zhou [a,b], Baihai Zhang [a], Kai Lin [b], Daming Xu [b], Caiwen Chen [b], Xinting Yang [b,*], Chuanheng Sun [b,*]

[a] School of Automation, Beijing Institute of Technology, Beijing 100081, China
[b] National Engineering Research Center for Information Technology in Agriculture, Beijing 100097, China

ARTICLE INFO

Article history:
Received 7 January 2017
Received in revised form 12 February 2017
Accepted 14 February 2017
Available online 24 February 2017

Keywords:
Aquaculture
Near-infrared image
Flocking index of fish feeding behavior
Delaunay Triangulation
Image analysis

ABSTRACT

In aquaculture, fish feeding behavior under culture conditions holds important information for the aquaculturist. In this study, near-infrared imaging was used to observe feeding processes of fish as a novel method for quantifying variations in fish feeding behavior. First, images of the fish feeding activity were collected using a near-infrared industrial camera installed at the top of the tank. A binary image of the fish was obtained following a series of steps such as image enhancement, background subtraction, and target extraction. Moreover, to eliminate the effects of splash and reflection on the result, a reflective frame classification and removal method based on the Support Vector Machine and Gray-Level Gradient Co-occurrence Matrix was proposed. Second, the centroid of the fish was calculated by the order moment, and then, the centroids were used as a vertex in Delaunay Triangulation. Finally, the flocking index of fish feeding behavior (FIFFB) was calculated to quantify the feeding behavior of a fish shoal according to the results of the Delaunay Triangulation, and the FIFFB values of the removed reflective frames were fitted by the Least Squares Polynomial Fitting method. The results show that variations in fish feeding behaviors can be accurately quantified and analyzed using the FIFFB values, for which the linear correlation coefficient versus expert manual scoring reached 0.945. This method provides an effective method to quantify fish behavior, which can be used to guide practice.

1. Introduction

The fish feeding process is one of the most important aspects in managing aquaculture tanks, where the cost of fish feeding is around 40% of the total production costs (Atoum et al., 2015; Chang et al., 2005). The inefficiencies of the feeding task associated with intensively cultured fish systems result in considerable financial loss for aquaculturists and negative environmental impact. So the efficient feeding strategies are very important (Føre et al., 2011; Wu et al., 2015). Information about the feeding behavior would be a valuable input into the process of developing efficient feeding management strategies, it holds important information for aquaculturist. Methods of continuously monitoring and quantifying the behavior of fish show potential for assessing the feeding process, and it reflects the fish feeding status and is important to fish production and culture (Kristiansen et al., 2004; McFarlane et al., 2004; Saberioon et al., 2016; M. Sun et al., 2016; Xu et al., 2006; Zion, 2012).

Many attempts have been made to monitor and analysis the process of fish behavior. Human observers can develop a capacity for evaluating the behavior of fish, but visual observation is often impeded by several factors such as the observer's experience. And so, for a commercial scale fish farm, raises labor and time costs, leading to the issue of how to quantify feeding behavior by a objective and automatic method (Liu et al., 2014; Mallekh et al., 2003). A high-frequency imaging sonar (DIDSON) and some acoustic tags were applied to directly observe and quantify fish behavior (Føre et al., 2011; Kolarevic et al., 2016; Rakowitz et al., 2012). Moreover, although acoustic techniques can be used without light, the application of these techniques is limited by the high cost and difficulty of implementation (Belcher et al., 2002; Saberioon et al., 2016; Zion and Barki, 2012).

Computer vision technology provides an automated, non-invasive and cost-effective method of recording behavioral parameters (Xu et al., 2006). In order to quantify the behavior, a behavior detection method based on computer vision and Delaunay Triangulation was developed by Nasirahmadi et al. (2017, 2015). And the classification of animal behavior was studied using machine vision and Support Vector Machine (SVM) (Martiskainen et al., 2009; Smith et al., 2016). Single camera or multi-camera 3D

* Corresponding authors.
E-mail address: sunch@nercita.org.cn (C. Sun).

http://dx.doi.org/10.1016/j.compag.2017.02.013
0168-1699/

machine vision has been used in behavior analysis or trail tracking (Saberioon and Cisar, 2016; Sadoul et al., 2014). Furthermore, a series of swimming, grouping behaviors monitoring and analyzing systems have been developed (Papadakis et al., 2012; Pinkiewicz et al., 2011). For feeding and related studies, machine imaging had been used previously to detect the feed residue in fish shoal feeding (Atoum et al., 2015; Foster et al., 1995; Parsonage and Petrell, 2003), quantify fish activity (Duarte et al., 2009), quantify feeding activity and behavior (Liu et al., 2014; Pinkiewicz et al., 2011), and estimate feeding intensity (Zhao et al., 2016). Practice has proven that machine vision is a highly cost-effective method and more suitable for an environment with sufficient lighting such as in a laboratory, cages, and pools (Dios et al., 2003; Kane et al., 2004; Saberioon et al., 2016; Xiao et al., 2015). While in some aquaculture facilities have poor lighting, the near-infrared computer vision technology is not affected by visible light intensity and can yield good imaging results in an environment with relatively dim light (Farokhi et al., 2016; Hung et al., 2016). Furthermore, the cost of this technique is also very low and the development is easy. Therefore, due to the low cost and low need of visible light intensity, it is suitable for used for motoring fish behaviors in aquaculture which have poor lighting. In fact, a near-infrared (NIR) system has already been deployed and achieved very good results for 3D fish movement trail tracking (Pautsina et al., 2015). In this study, according to the study of Pautsina et al. (2015), a 850 nm wavelength near-infrared was used, and this wavelength has not been shown to affect normal fish growth or result in a stress response.

On the basis of simulating the commercial scale fish farm environment, the current study proposed a near infrared computer vision-based method for quantify the feeding behavior of fish. Feeding behavior was described by the flocking level based on a Delaunay Triangulation method due to the motions of feeding fish. Meanwhile, possible factors that might influence the analysis results were both taken into account, including water surface reflections were classified by the SVM. To assess the reliability of our method, it was also compared with the results of human exports method. The purpose of this study was to build a potential method to quantify the feeding behavior of swimming fishes. It aims to provide information for real time feedback and automatically control of feeding process in fish feeding procedures.

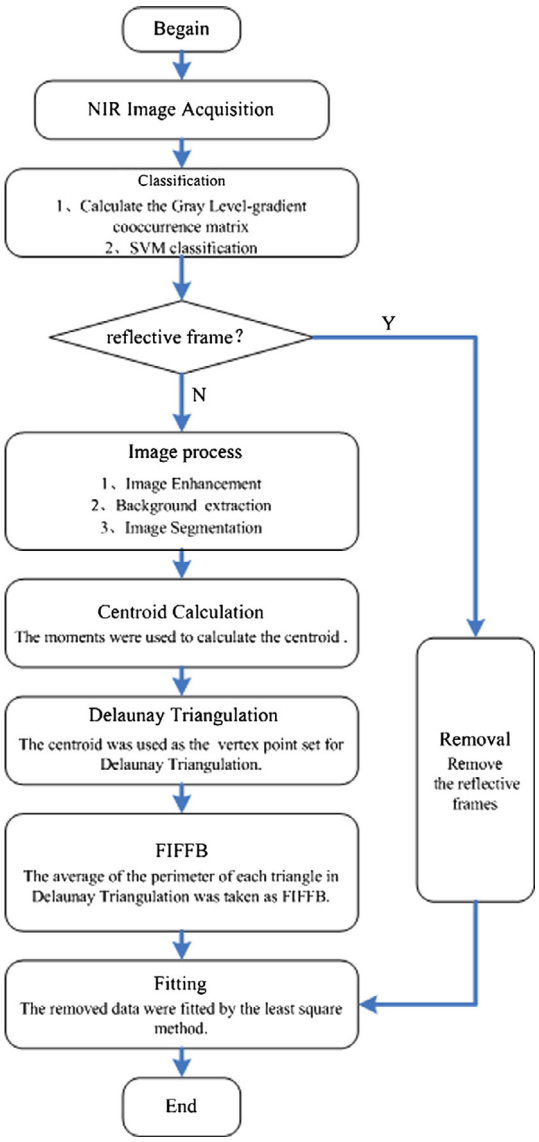

Fig. 1. Schematic of the near-infrared imaging method.

2. Materials and methods

In this study, the method is not suitable for all fish species or culture methods, the preconditions for the method proposed in this paper are indicated as follows:

(1) Species. By default, this method is applicable to swimming fish species such as carp, salmon, and tilapia, which feed actively and have significantly different feeding behaviors at different life stages.
(2) Feeding mode. The suitable fish feeding methods include manual feeding or fixed-point feeding from a feeder; floating and sinking types of feed are acceptable.
(3) Culture pattern. This method is suitable for cages, ponds, and RAS, and it is highly recommended for use in environments with poor light conditions.

A schematic of the system is shown in Fig. 1.

2.1. Experimental materials

For this experiment, adult *Cyprinus carpio var. specularis* fish of 15–25 cm in length were selected as the subjects. Before being used in the experiment, the fish were raised for several months and were allowed to adapt to the experimental culture environment. During acclimation, the oxygen level was maintained within the range of 5–7 mg/L, water temperature was maintained at 15–27 °C, and the fish were fed a commercial diet of 3% of the body weight per day.

2.2. Experimental system

The experiment was performed in the aquaculture laboratory at the Xiaotangshan National Experiment Station for Precision Agriculture, Beijing, China. The system includes six tanks, each with a diameter of 1.5 m and a water depth of 1 m. A Mako G-223B NIR industrial camera (Germany AVT, Allied Vision Technologies) was used for image collection; the camera had a bit depth of 8\12, a pixel dimension of 5.5 μm, and a resolution of 2048 * 1088. It was used in conjunction with a near-infrared light source of 850 nm and an industrial camera lens with a focal length of 8 mm (KOWA LM8HC, Japan). The total photon flux at the water surface was 57.8 μmol m^{-2} s^{-1}. The camera and the near-infrared light source were attached to the top of the tank. Since the distance

from the camera to the water surface is an important data because a short distance can distort the obtained image, while a long distance will be reduce the area of the active area. In this study, the distance was determined as 1.5 m experimentally based on the testing of the system, and this value allows monitoring most of the water volume of the tank. The position of the light compensation lamp was adjusted so that the light was reflected in the same direction as the water outlet of the tank. A computer (Intel® Core™ i5-4590 CPU@3.30 GHz, 4.00 GB RAM) was used to collect near-infrared images in real-time and to analyze the resulting images. In order to reduce the abnormal behavior of the fish caused by human activities, the computer was placed in the control room next to the laboratory and connected to the camera via a 30-m twisted-pair gigabit cable. Image processing was implemented in MATLAB® software (The MathWorks Inc., Natick, MA, USA). And the regular feeding was performed via the feeder. The experimental equipment is illustrated below in Fig. 2.

To prevent bubbles from the oxygenation device affecting the image processing, an air blower was used for biological filter aeration, which significantly reduced the amounts of foam and bubbles and their effects on the imaging results (Liu et al., 2014). In order to prevent the fluctuation of the water surface, the water inlet was submerged below the water surface, and the water flow enters into the tank along the tangential direction.

2.3. Image processing

2.3.1. Reflective frame classification

In aquaculture, reflections are always present in images, particularly due to fluctuations caused by fish feeding and fighting for food. Fig. 3a shows an extreme case of reflection. It can be seen that target and other details were completely submerged in the area, and this situations may lead to calculation errors and deviation. Therefore, the reflective frames should be detected and processed to guarantee the accuracy and precision of the processing result. And the reflective frames can be divided into two categories, the first category images include relatively fixed reflection points such as the light source, tank wall, and water outlet. The reflections from these images can be removed via background subtraction. The second category image is caused by fish activity, surface flow fluctuation, and bubbles. This category is able to bring the error, and the removal of reflective frames cannot be easily determined whether there is a reflection point. In this study, the reflective frames were classified by the Support Vector Machine (SVM), and the texture features were extracted by a Gray-Level Gradient Co-occurrence Matrix (GLGCM).

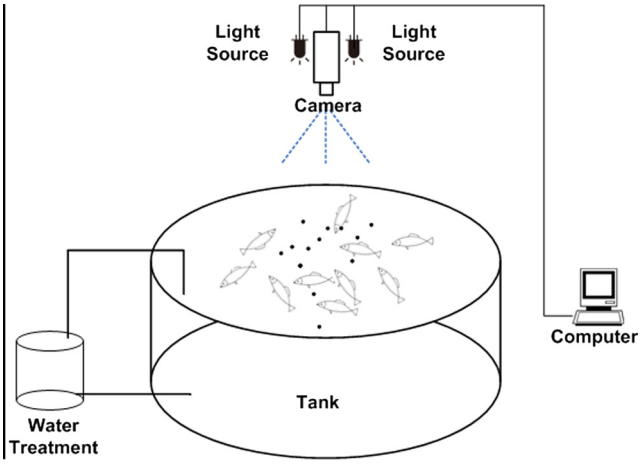

Fig. 2. Diagram of the experimental system.

When there is a reflection in the frame, the texture of the image will have a great change, as show in the 3D gray level map of reflective frame (Fig. 3b), the fluctuation area of the gray-level change is more intense, and the pixel gradient value rises sharply (Fig. 3c). Therefore, the image texture can measure the reflectivity to a certain extent, and a GLGCM was introduced to represent this change (Hong, 1984; Pu et al., 2015; Xiong et al., 2015). The GLGCM model reflects the relation between the gray level and the gradient (or edge) of the pixel in the image. The gray level of each pixel is the basis of an image, whereas the gradient is the contour of the edge of the image elements. The gray-level gradient space can express the gray-level and gradient-distribution regularity of the pixels in the image, which can depict the texture well, and the reflectivity can be better described.

After the GLGCM was constructed in each image, a set of 15 features were calculated: (1) small gradient strengths, (2) large gradient strengths, (3) inhomogeneity of grayscale distribution, (4) inhomogeneity of grayscale-gradient distribution, (5) energy, (6) grayscale mean, (7) mean gradient, (8) mean square error of grayscale, (9) mean square error of grayscale gradient, (10) correlation, (11) grayscale entropy, (12) gradient entropy, (13) entropy of mixing, (14) inertia, and (15) inverse difference moment. Based on the above features, the SVM (Chen et al., 2010; Cortes and Vapnik, 1995; Hu et al., 2012) was then used to classify these images to determine whether the frame should be removed. Given that the flocking index of fish feeding behavior (FIFFB) calculation relies on the distribution of individual fish and requires a minimal sample, too few samples will have an unfavorable effect on the calculation result. Therefore, the reflective frame removal was converted into an identification-rate calculation problem. Then, 100 images of each type were randomly selected by human observation, among these, the second category images always had bad visual effects, and the identification rate calculated by the human observation was less than p. In this paper, p was chosen as 90%. Such a frame may be considered a frame that should be removed. The GLGCM was taken as the extracted feature data, 90% of the images were taken as training data, and the remaining 10% were taken as test data. The SVM was trained and tested. The SVM classifier was realized by using a library for support vector machines (LIBSVM) (Chang and Lin, 2011), and the RBF kernel was used as the kernel function. Among the images, the selection of parameters c (cost) and g (gamma) of the LIBSVM is key to classification accuracy. In this paper, the cross-validation and grid search method were used to achieve the optimal parameters (Picard and Cook, 1984). The new data interpolation method after reflective frame removal is elaborated in Section 2.4.4.

2.3.2. Contrast enhancement

Most species of fish can change skin color to adapt to the ambient color (Fujimoto et al., 1991; Papoutsoglou et al., 2000; Xu et al., 2006). Therefore, in order to obtain excellent segmentation results, the image should be enhanced to improve the contrast between the target and image background. In this paper, the Multi-Scale Retinex (MSR) algorithm was used to enhance the images (Land and McCann, 1971), This method effectively improves the gray level and contrast and displays the details that are hidden in shadowed or illuminated areas. The MSR algorithm is shown as Eq. (1):

$$\mathrm{R}(x,y) = \sum_{k=1}^{M} \omega_k \{\log[I(x,y)] - \log[F(x,y,c_k) \otimes I(x,y)]\} \quad (1)$$

where the original image is I(x,y); the reflected image is R(x,y); c_k is the scale, $F(x,y,c_k)$ is the center/surround function; $\otimes$ denotes the convolution; and k is the quantity of the Gaussian center/surround functions and determined by the normalization condition $F(x,y,c) = 1$. Normally, M is set to 3, and $w_1 = w_2 = w_3 = 1/3$ (G. Sun

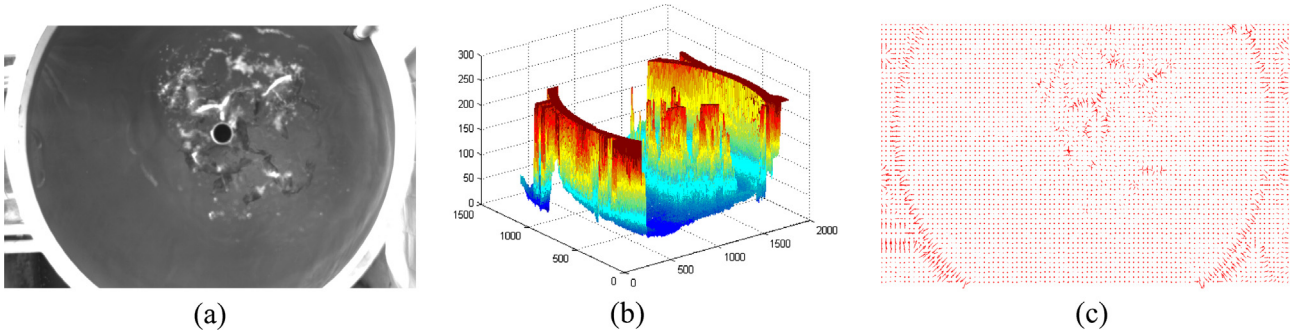

Fig. 3. Reflection frame. (a) Original image; (b) gray level 3D map; and (c) gradient vector map.

et al., 2016). As shown in the images, the result after enhancement is shown in Fig. 4b. In comparison with the original image (Fig. 4a), uneven light and the effects of changes are eliminated, the details of the dark area is highlighted, and the contrast of the image is improved.

2.3.3. Target extraction

In the near-infrared image, the fish were brighter than the water tank reflection. This characteristic can be used to remove fish and obtain the background. According to the average background method (Downey and Koutsopoulos, 1993) and background subtraction. The background and fish bodies were extracted (Figs. 4c and d). However, when fish swim in a tank, overlapping is inevitable. Based on the principle that a fish's body is a smooth curve, a watershed algorithm (Beucher, 1982; Beucher and Lantuéjoul, 1979) was used to segment concatenated images to obtain the image of a single fish. Next, the target was filtered based on the fish's body size to exclude objects that were too small or large and to obtain a binary image.

2.4. Analyzing and extracting feeding behavior characteristics

2.4.1. Fish body centroid calculation

In this study, the image collection equipment was installed at the top of the tank. The captured image can be viewed as a horizontal plane, and the target can be viewed as the area of a pixel area of the water surface. This study focuses on the development rules of movement in this area to analyze the area and extract the centroid to represent the rough position of the fish. For a two-dimensional image, centroid calculation can be viewed as a calculation process that assigns a weight to the gray level of all pixels in the target image. Physically, this can be viewed as a process for calculating the moment for a discretized digital image: the centroid is the 0th and 1st order moments (Moreda et al., 2012). In this paper, the target pixel area is a discretized image, and the target centroid was calculated via the 0th order moments. For the target image, the moments are represented below in Eq. (2).

$$m_{pq} = \sum_{j-1}^{N}\sum_{i-1}^{N} i^p j^q f(i,j) \tag{2}$$

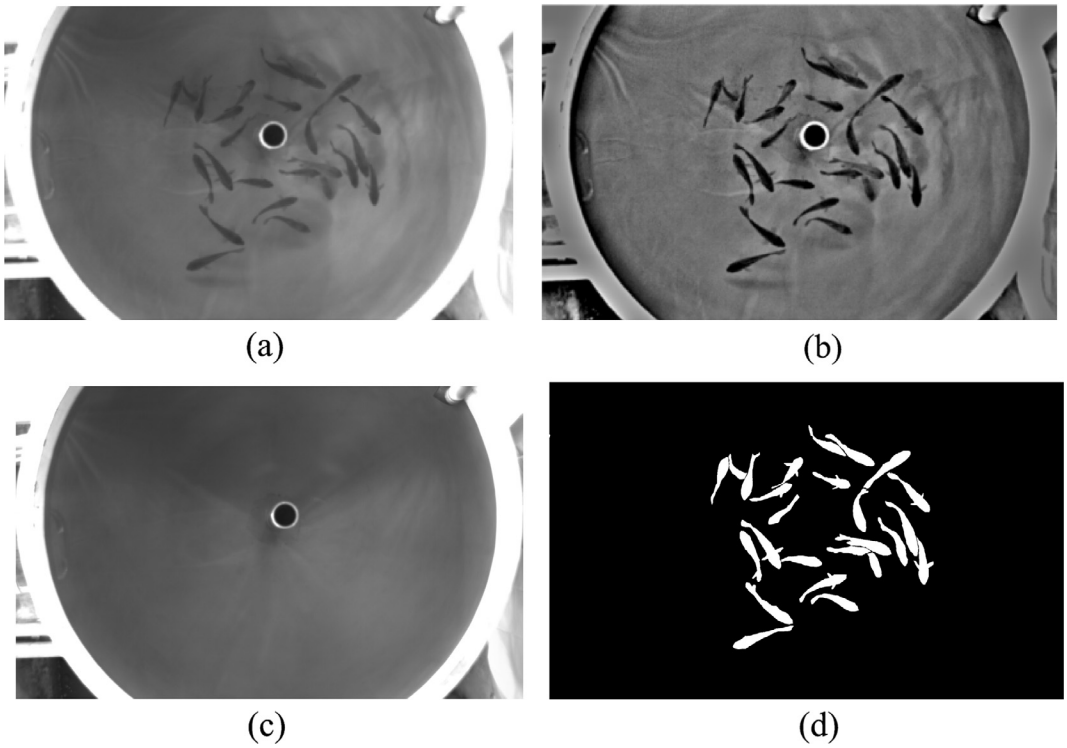

Fig. 4. NIR image. (a) Original image; (b) image enhancement result; (c) background; and (d) binary image.

where p and q are orders; and i and j are image pixel indexes. The target centroid coordinates (x_c,y_c) are represented below in Eq. (3).

$$x_c = \frac{m_{10}}{m_{00}}, \quad y_c = \frac{m_{01}}{m_{00}} \tag{3}$$

The fish centroid in a binary image was calculated via the Eq. (3), and the result is shown in Fig. 5b.

2.4.2. Delaunay triangulation

Delaunay Triangulation defines triangles formed from a point set P in the plane. The circumcircle is the only circumcircle that crosses the three vertices of a triangle; the vertex is not inside any circumcircle, and none of the four points can be concyclic. Among all possible triangulations of a scattered point set, a triangle from Delaunay Triangulation has the largest minimal angle (Thiessen, 1911). In this study, a triangulation growth algorithm was used for triangulation (Brassel and Reif, 1979). For a planar point set P in which no four points in the same circle Pi denote the ith point in point set P, E is the list of edges to be extended, and T is a list of triangles. Based on this rule, the Delaunay Triangulation process is as follows:

(1) One point P_1 was selected randomly from the scattered point set; the point P_2 closest to P_1 was identified. These two points were connected to form an edge defined as P_1P_2, i.e., a Delaunay edge.
(2) Based on edge P_1P_2, the third point P_3 in the point set was identified that satisfied the Delaunay rule and resulted in a circumcircle with the minimum radius. Triangle $\triangle P_1P_2P_3$ was the initial Delaunay triangle.
(3) The other two edges P_1P_3 and P_2P_3 of $\triangle P_1P_2P_3$ were added to the candidate extension edge list E, and triangle $\triangle P_1P_2P_3$ was added to the triangle list T, as shown in Fig. 5a.
(4) When the candidate extension edge list E was nonempty, the iteration was performed according to the aforementioned method until all baselines were processed.

In this paper, the centroids of the fish body are defined as point set P to Delaunay Triangulation. Based on the aforementioned algorithm, the image after Delaunay Triangulation is shown below in Fig. 5c.

2.4.3. Calculation of the feeding behavior quantification factor FIFFB

In a Delaunay triangle, the three vertices of each triangle correspond to the minimal circumcircle. Therefore, each triangle's size reflects the distance between vertices. For a shoal of fish in multiple images, the average triangle perimeter reflects the aggregation level. In a Delaunay triangle, the FIFFB for a shoal of fish in multiple images is represented as Eq. (4):

$$\mathrm{FIFFB} = \frac{\sum_{i=1}^{n} P_i}{n} = \frac{\sum_{i=1}^{n} (L_{i1} + L_{i2} + L_{i3})}{n} \tag{4}$$

where n is the number of Delaunay triangles; P_i is the perimeter of the i-th triangle; and L_{i1}, L_{i2}, and L_{i3} are the three edges of the triangle. The above definition shows that the FIFFB is the average perimeter of all triangles in a Delaunay Triangulation and represents the fish aggregation level. A smaller value corresponds to a higher fish aggregation.

2.4.4. Least square polynomial fitting of FIFFB

The second category images should be removed, and then, new data should be filled in. The problem becomes how to obtain the overall rule via calculating an unknown continuous function defined in the continuous set S (M is contained by S) when the constraints on the discrete point set M are known. Fitting is one solution for this approximate relation. The data in this study were calculated and include errors. If the obtained approximation function must cross all points accurately without error, the curve will retain all the test errors. Fitting does not require that all data points be included in the fitting curve, and the obtained curve has a functional relation. This result was obtained by substituting the required data points. In this paper, the corresponding value was derived via least square fitting because the reflective frame images that should be removed were inconsistent.

In a series of images, the n consecutive images were assumed to be reflective frames; therefore, the FIFFBs of these n images could not be calculated or were calculated with error. If it is assumed that the function $f_{FIFFB}(x)$ corresponds to n images, then $f_{FIFFB}(x)$ = FIFFB $(x)(i = 1, 2, \ldots, n)$. If the fitting polynomial is $y = a_0 + a_1x + \cdots + a_kx^k$, the coefficient matrix A = [a_0, a_1, . . . , a_k] can be obtained by minimizing the value of $\min_{\varphi} \sum_{i=1}^{m} \delta^2 = \sum_{i=1}^{m} (f(x_i) - y_i)^2$. Therefore, the function $f_{FIFFB}(x)$ was obtained via fitting. After the function was defined, the least square polynomial fitting was performed based on the data from the frames adjacent to the reflective frame. Next, the removed reflective frame position was substituted into the function to obtain the new interpolated FIFFB for this position. Based on the above curves, the FIFFB of n frames can be calculated.

3. Results and discussion

3.1. Reflective frame classification

In this paper, 100 images were selected as the samples from each type, among which 180 images were used as training data for the SVM, and the 20 remaining images were used as test data. Finally, after training and testing had been performed, the SVM classifier's optimal parameters cost c and kernel function parameter g was selected. Fig. 6 shows the 3D view contour map of the

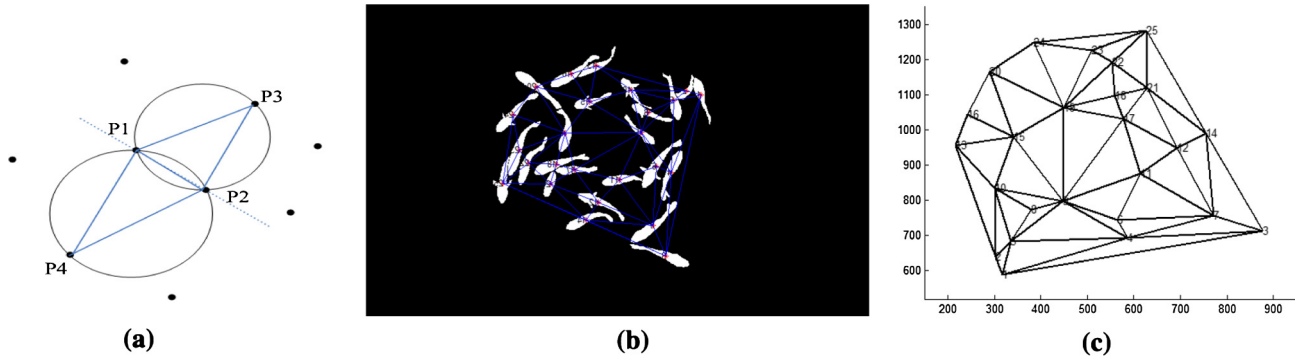

Fig. 5. Delaunay triangulation. (a) Initial Delaunay triangle; (b) Set P; and (c) result.

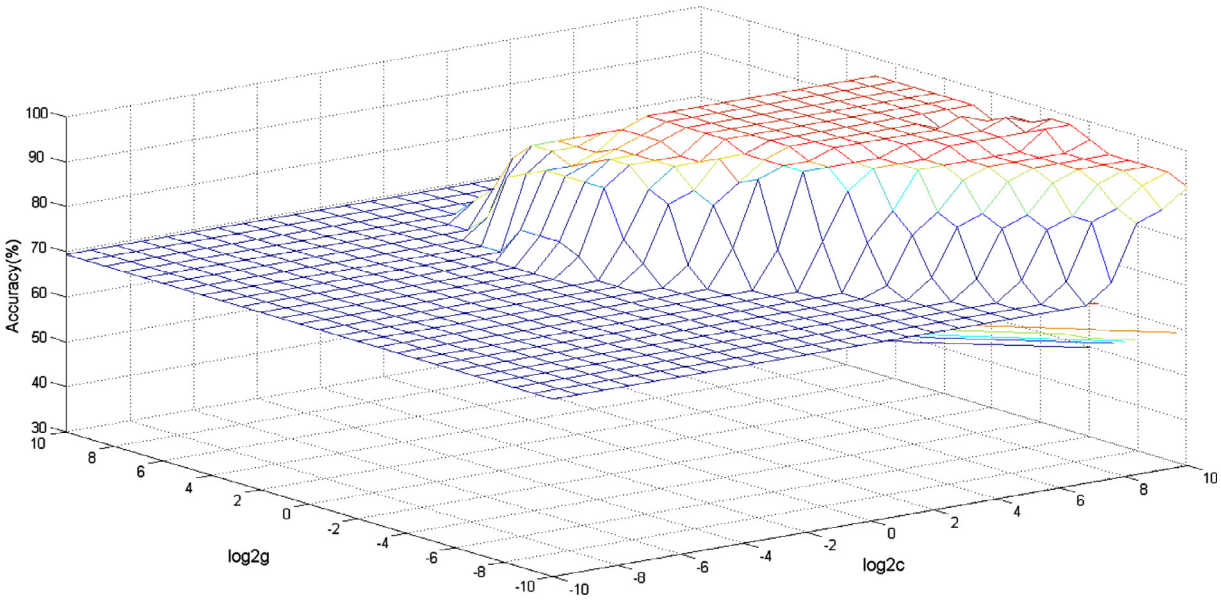

Fig. 6. The 3D view contour map of the SVM parameter selection.

SVM parameter selection process. The range of parameters c and g are set to $[2^{-10},2^{10}]$ and $[2^{-10},2^{10}]$ respectively, and the change step length of c and g are set to 0.5. From the figure it can be seen when the parameters were selected as c = 8 and g = 0.088, the optimal accuracy of the SVM classification can reach 97.96%. Therefore, the SVM can be used to achieve the classification of reflective frames, and it also provides a practical method to remove the reflective frame.

3.2. Fish target recognition results

The recognition rate of fish determined the accuracy of the method. The recognition rate was calculated by comparing the number of analyzed fish with the actual number of fish for two tanks (No. 1 and No. 2), using images that were taken on 10 consecutive days at 1200 frames per day (20 min per day, one frame per second). The results showed that the proposed algorithm achieves a recognition rate of 92.995 (± 1.4)% (Table 1). Many reasons exist for these errors. For example, the camera lens was exposed to the damp environment for a long time, and the water mist on the lens reduced the recognition rate; furthermore, the fish were not completely segmented or were over-segmented due to cross-overlapping. In addition, an algorithm should be applied to account for these problems. Additionally, the authors believe that the method presented in this paper will achieve better accuracy for fish with scales and high-contrast color, which requires verification in future studies.

3.3. FIFFB variation rule

To facilitate observation of the variation of the FIFFB, images at t = 5, 15, 30, and 60 were first selected to represent the states of the fish before, during, and after feeding. Fig. 7 shows images with the respective Delaunay Triangulation at four different moments. From this figure it can be seen that the FIFFB of each triangle was different at four different moments during the feeding. The FIFFB was smaller at t = 15 and t = 30 than at other moments, indicating that fish had more flocking during feeding time, while at t = 5 and t = 60 the FIFFB declined and fish were satisfied and scattered. Therefore this feature can be used for quantify the flocking level in the Delaunay Triangulation and indicates that the output could be used for assessing the feeding activities.

In order to describe the feeding process more accurately, the FIFFB during the entire feeding process should be calculated. In February 2017, a fish feeding experiment was performed in the laboratory. When the experiment began, feeding was provided three times at 30-min intervals. The feeding time started from t = 10 s at each feeding time until a fair amount of food was floating on the surface, the fish were swimming around, and they had stopped feeding. At this point, the residual food was removed, and feeding was stopped. The reflective frame was classified by the SVM, according to the classification results, frame 11 to frame 18 is considered to be the second type of reflective frame. After the above reflective frames are removed, the data is added using the least-squares fitting method, the process shown in Fig. 8, the solid line represents the original FIFFB values, the dashed dotted line corresponds to the fitted values.

The position of the reflective frame was substituted into the fitting polynomial function to obtain new FIFFB data and to plot the FIFFB trend curve for each feeding event (Fig. 9).

Fig. 9 shows that the FIFFB was essentially stable with little fluctuation when t < 10. Starting from the initial feeding at t = 10 s, the results show that the three FIFFB curves decreased rapidly because the fish were fighting for food, which results in a short aggregation period. When the FIFFB reached the minimum value, it remained relatively stable and then increased gradually until it reached the state before feeding. At the same time, feeding had stopped, the fish swam away, and the aggregation level

Table 1
Recognition rate.

Day		1	2	3	4	5	6	7	8	9	10
Recognition rate (%)	No.1 Tank	92.6	93.4	91.6	93.2	94.3	92.5	92.5	93.6	92.8	93.0
	No.2 Tank	92.9	93.1	92.9	93.3	93.8	93.7	92.7	93.6	93.8	92.6

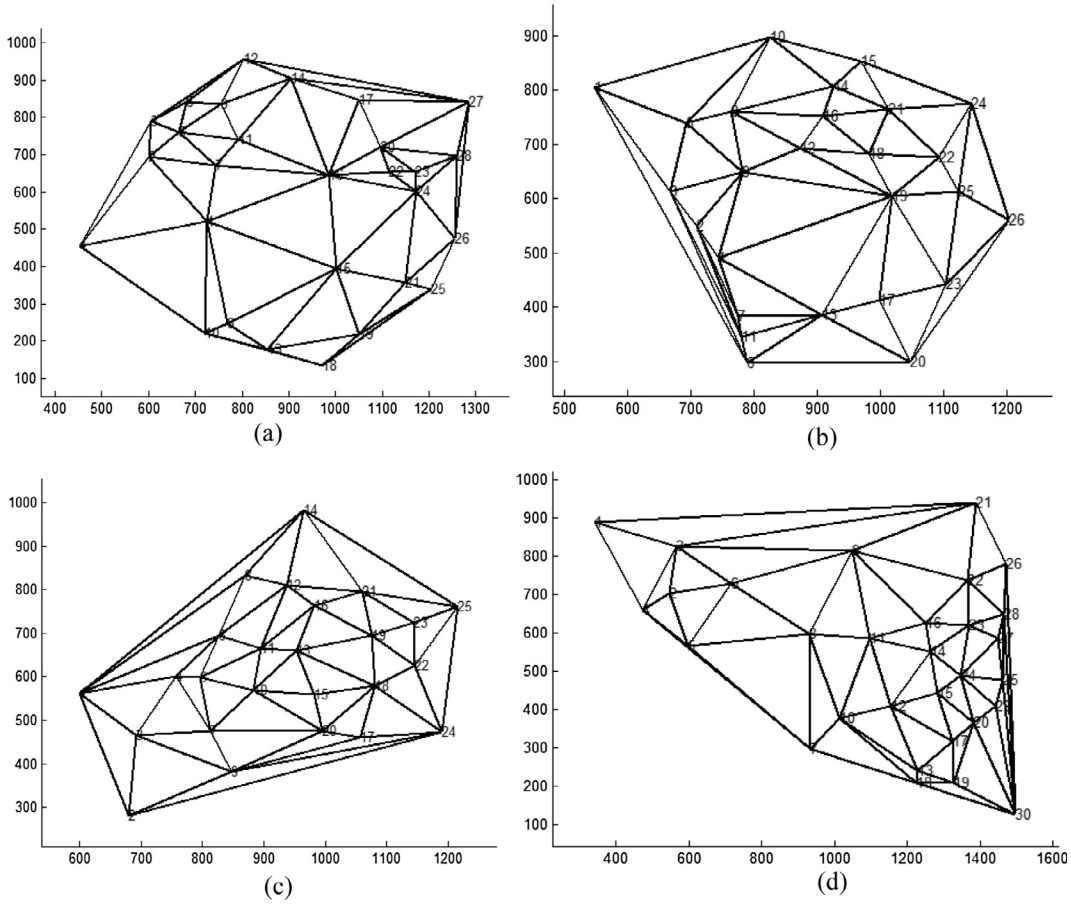

Fig. 7. The FIFFBs at selected moments. (a) t = 5, FIFFB = 527.7593; (b) t = 15, FIFFB = 438.66; (c) t = 30, FIFFB = 436.23; and (d) t = 60, FIFFB = 610.27.

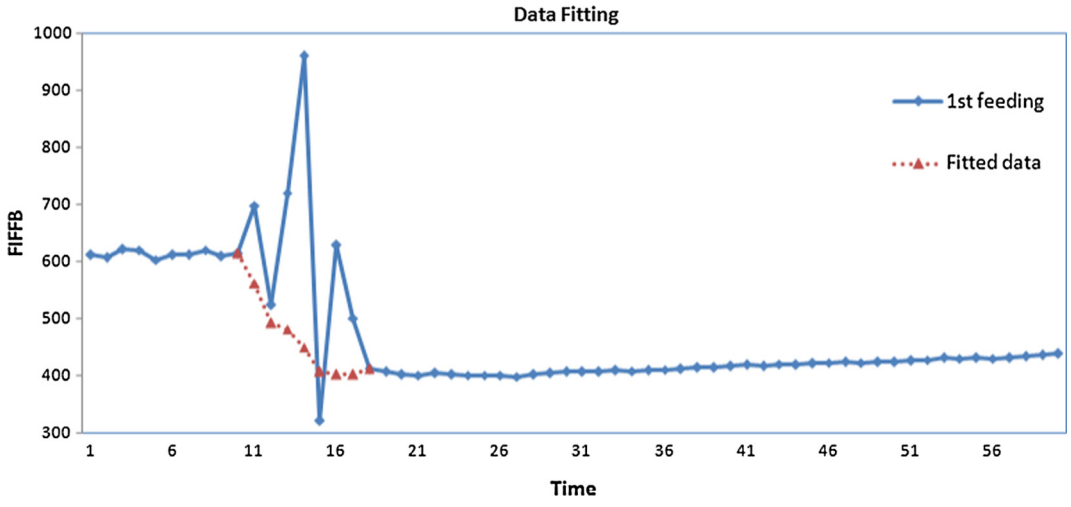

Fig. 8. A typical fitting processing of FIFFB.

decreased. During the three rounds of consecutive feeding, feeding at the later stage always resulted in the faster recovery of the original FIFFB level. This finding shows that the fishes' appetites were not as strong after one or two rounds of feeding, and this also consistent with the conclusions obtained by other researchers (Wyatt, 1972). Fig. 9 shows that the FIFFB accurately describes the changes in the behaviors of fish during feeding, which also proves the above conclusions.

3.4. FIFFB correlation analysis

For further verification of whether the FIFFB can be used to quantify changes in feeding behavior, the correlations between the FIFFB and the manual expert method should be analyzed. For this comparison, frames of the feeding images were extracted every 10 s, and 10 individuals were asked to evaluate and score the feeding intensity. The 10 individuals were consisted of 4

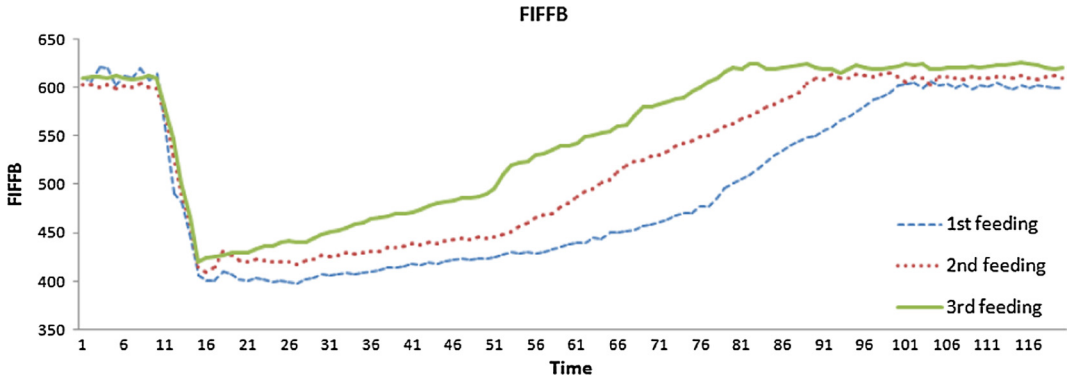

Fig. 9. FIFFB curves.

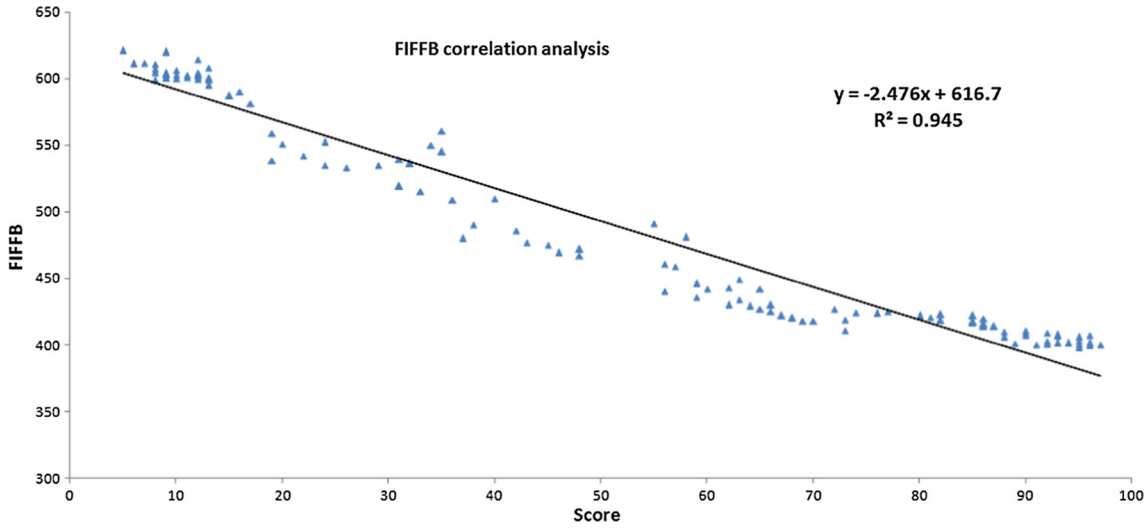

Fig. 10. Correlation between the FIFFB and human expert observations.

experienced researchers and 6 operating professionals. The feeding intensity was scored from 0 to 100, with 0 corresponding to no feeding and 100 corresponding to violent fighting for food. Each image was scored to obtain 10 data points. After the maximum and minimum values were removed, the average value was used as the score for the image. Linear correlation analysis of these values with the FIFFB resulted in a linear correlation coefficient of 0.945 (Fig. 10). This result means that the FIFFBs calculated by using this method were highly correlated with the human expert observation.

4. Conclusions

In conclusion, it was shown that the developed method can accurately describe fish feeding behavior and achieves desirable results because the linear correlation coefficient obtained from comparing the results from the manual and FIFFB methods reached 0.945. Therefore this method could contribute in the future as an important and economically feasible technique in commercial fish farms for assessment of fish feeding process. This is an important step towards the development of an automated feeding system that can realize the real time feedback and control of feeding process.

However this method needs more study for a larger sample size and future development of a method for extracting features in an area in order to represent the feeding group behavior for a high-density and large population group. Finding the best solutions for environmental challenges like moist vapor which cover camera lenses with fog and reduced visibility needs to be investigated before the technique can be implemented in commercial fish farms.

Acknowledgments

The research in this paper was supported by the National Key Technology R&D Program of China (2015BAD17B04) and the Beijing Natural Science Foundation (6152009).

References

Atoum, Y., Srivastava, S., Xiaoming, L., 2015. Automatic feeding control for dense aquaculture fish tanks. IEEE Sig. Process. Lett. 22, 1089–1093.
Belcher, E., Hanot, W., Burch, J., 2002. Dual-Frequency Identification Sonar (DIDSON). In: Proceedings of the 2002 International Symposium on Underwater Technology (Cat. No. 02EX556), pp. 187–192.
Beucher, S., 1982. Watersheds of functions and picture segmentation, Acoustics, Speech, and Signal Processing. In: IEEE International Conference on ICASSP '82, pp. 1928–1931.
Beucher, S., Lantuéjoul, C., 1979. Use of Watersheds in Contour Detection. In: International Workshop on Image Processing, Real-Time Edge and Motion Detection, pp. 391–396.
Brassel, K.E., Reif, D., 1979. A procedure to generate Thiessen polygons. Geograph. Anal. 11, 289–303.
Chang, C.-C., Lin, C.-J., 2011. LIBSVM: a library for support vector machines. ACM Trans. Intell. Syst. Technol. 2, 1–27.
Chang, C.M., Fang, W., Jao, R.C., Shyu, C.Z., Liao, I.C., 2005. Development of an intelligent feeding controller for indoor intensive culturing of eel. Aquacult. Eng. 32, 343–353.

Chen, K., Sun, X., Qin, C., Tang, X., 2010. Color grading of beef fat by using computer vision and support vector machine. Comp. Electron. Agricult. 70, 27–32.
Cortes, C., Vapnik, V., 1995. Support-Vector Networks. Mach. Learn. 20, 273–297.
Dios, M.D., Serna, C., Ollero, A., 2003. Computer vision and robotics techniques in fish farms. Robotica 21, 233–243.
Downey, A.B., Koutsopoulos, H.N., 1993. Primitive-based classification of pavement cracking images. J. Transport. Eng. 119, 402–418.
Duarte, S., Reig, L., Oca, J., 2009. Measurement of sole activity by digital image analysis. Aquacult. Eng. 41, 22–27.
Føre, M., Alfredsen, J.A., Gronningsater, A., 2011. Development of two telemetry-based systems for monitoring the feeding behaviour of Atlantic salmon (Salmo salar L.) in aquaculture sea-cages. Comp. Electron. Agricult. 76, 240–251.
Farokhi, S., Flusser, J., Ullah Sheikh, U., 2016. Near infrared face recognition: a literature survey. Comp. Sci. Rev. 21, 1–17.
Foster, M., Petrell, R., Ito, M.R., Ward, R., 1995. Detection and counting of uneaten food pellets in a sea cage using image analysis. Aquacult. Eng. 14, 251–269.
Fujimoto, M., Arimoto, T., Morishita, F., Naitoh, T., 1991. The background adaptation of the flatfish, Paralichthys olivaceus. Physiol. Behav. 50, 185–188.
Hong, J., 1984. Gray level-gradient co-occurrence matrix texture analysis method. Acta Autom. Sin. 10, 22–25.
Hu, J., Li, D., Duan, Q., Han, Y., Chen, G., Si, X., 2012. Fish species classification by color, texture and multi-class support vector machine using computer vision. Comp. Electron. Agricult. 88, 133–140.
Hung, C.-C., Tsao, S.-C., Huang, K.-H., Jang, J.-P., Chang, H.-K., Dobbs, F.C., 2016. A highly sensitive underwater video system for use in turbid aquaculture ponds. Scient. Rep. 6, 31810.
Kane, A.S., Salierno, J.D., Gipson, G.T., Molteno, T.C.A., Hunter, C., 2004. A video-based movement analysis system to quantify behavioral stress responses of fish. Water Res. 38, 3993–4001.
Kolarevic, J., Aas-Hansen, Ø., Espmark, Å., Baeverfjord, G., Terjesen, B.F., Damsgård, B., 2016. The use of acoustic acceleration transmitter tags for monitoring of Atlantic salmon swimming activity in recirculating aquaculture systems (RAS). Aquacult. Eng. 72–73, 30–39.
Kristiansen, T.S., Fernö, A., Holm, J.C., Privitera, L., Bakke, S., Fosseidengen, J.E., 2004. Swimming behaviour as an indicator of low growth rate and impaired welfare in Atlantic halibut (Hippoglossus hippoglossus L.) reared at three stocking densities. Aquaculture 230, 137–151.
Land, E.H., McCann, J.J., 1971. Lightness and retinex theory. J. Opt. Soc. Am. 61, 1–11.
Liu, Z., Li, X., Fan, L., Lu, H., Liu, L., Liu, Y., 2014. Measuring feeding activity of fish in RAS using computer vision. Aquacult. Eng. 60, 20–27.
Mallekh, R., Lagardère, J.P., Eneau, J.P., Cloutour, C., 2003. An acoustic detector of turbot feeding activity. Aquaculture 221, 481–489.
Martiskainen, P., Järvinen, M., Skön, J.-P., Tiirikainen, J., Kolehmainen, M., Mononen, J., 2009. Cow behaviour pattern recognition using a three-dimensional accelerometer and support vector machines. Appl. Anim. Behav. Sci. 119, 32–38.
McFarlane, W.J., Cubitt, K.F., Williams, H., Rowsell, D., Moccia, R., Gosine, R., McKinley, R.S., 2004. Can feeding status and stress level be assessed by analyzing patterns of muscle activity in free swimming rainbow trout (Oncorhynchus mykiss Walbaum)? Aquaculture 239, 467–484.
Moreda, G.P., Muñoz, M.A., Ruiz-Altisent, M., Perdigones, A., 2012. Shape determination of horticultural produce using two-dimensional computer vision – a review. J. Food Eng. 108, 245–261.
Nasirahmadi, A., Hensel, O., Edwards, S.A., Sturm, B., 2017. A new approach for categorizing pig lying behaviour based on a Delaunay triangulation method. Animal 11, 131–139.
Nasirahmadi, A., Richter, U., Hensel, O., Edwards, S., Sturm, B., 2015. Using machine vision for investigation of changes in pig group lying patterns. Comp. Electron. Agricult. 119, 184–190.
Papadakis, V.M., Papadakis, I.E., Lamprianidou, F., Glaropoulos, A., Kentouri, M., 2012. A computer-vision system and methodology for the analysis of fish behavior. Aquacult. Eng. 46, 53–59.
Papoutsoglou, S.E., Mylonakis, G., Miliou, H., Karakatsouli, N.P., Chadio, S., 2000. Effects of background color on growth performances and physiological responses of scaled carp (Cyprinus carpio L.) reared in a closed circulated system. Aquacult. Eng. 22, 309–318.
Parsonage, K.D., Petrell, R.J., 2003. Accuracy of a machine-vision pellet detection system. Aquacult. Eng. 29, 109–123.
Pautsina, A., Císař, P., Štys, D., Terjesen, B.F., Espmark, Å.M.O., 2015. Infrared reflection system for indoor 3D tracking of fish. Aquacult. Eng. 69, 7–17.
Picard, R.R., Cook, R.D., 1984. Cross-validation of regression models. J. Am. Statist. Assoc. 79, 575–583.
Pinkiewicz, T.H., Purser, G.J., Williams, R.N., 2011. A computer vision system to analyse the swimming behaviour of farmed fish in commercial aquaculture facilities: a case study using cage-held Atlantic salmon. Aquacult. Eng. 45, 20–27.
Pu, H., Sun, D.W., Ma, J., Cheng, J.H., 2015. Classification of fresh and frozen-thawed pork muscles using visible and near infrared hyperspectral imaging and textural analysis. Meat Sci. 99, 81–88.
Rakowitz, G., Tušer, M., Říha, M., Jůza, T., Balk, H., Kubečka, J., 2012. Use of high-frequency imaging sonar (DIDSON) to observe fish behaviour towards a surface trawl. Fish. Res. 123–124, 37–48.
Saberioon, M., Gholizadeh, A., Cisar, P., Pautsina, A., Urban, J., 2016. Application of machine vision systems in aquaculture with emphasis on fish: state-of-the-art and key issues. Rev. Aquacult., 1–19
Saberioon, M.M., Cisar, P., 2016. Automated multiple fish tracking in three-dimension using a structured light sensor. Comp. Electron. Agricult. 121, 215–221.
Sadoul, B., Evouna Mengues, P., Friggens, N.C., Prunet, P., Colson, V., 2014. A new method for measuring group behaviours of fish shoals from recorded videos taken in near aquaculture conditions. Aquaculture 430, 179–187.
Smith, D., Rahman, A., Bishop-Hurley, G.J., Hills, J., Shahriar, S., Henry, D., Rawnsley, R., 2016. Behavior classification of cows fitted with motion collars: decomposing multi-class classification into a set of binary problems. Comp. Electron. Agricult. 131, 40–50.
Sun, G., Li, Y., Wang, X., Hu, G., Wang, X., Zhang, Y., 2016. Image segmentation algorithm for greenhouse cucumber canopy under various natural lighting conditions. Int. J. Agricult. Biol. Eng. 9, 130–138.
Sun, M., Hassan, S.G., Li, D., 2016. Models for estimating feed intake in aquaculture: a review. Comp. Electron. Agricult. 127, 425–438.
Thiessen, A.H., 1911. Precipitation averages for large areas. Month. Weath. Rev. 39, 1082–1084.
Wu, T.-H., Huang, Y.-I., Chen, J.-M., 2015. Development of an adaptive neural-based fuzzy inference system for feeding decision-making assessment in silver perch (Bidyanus bidyanus) culture. Aquacult. Eng. 66, 41–51.
Wyatt, T., 1972. Some effects of food density on the growth and behaviour of plaice larvae. Mar. Biol. 14, 210–216.
Xiao, G., Feng, M., Cheng, Z., Zhao, M., Mao, J., Mirowski, L., 2015. Water quality monitoring using abnormal tail-beat frequency of crucian carp. Ecotoxicol. Environ. Safety 111, 185–191.
Xiong, Z., Sun, D.-W., Pu, H., Zhu, Z., Luo, M., 2015. Combination of spectra and texture data of hyperspectral imaging for differentiating between free-range and broiler chicken meats. LWT - Food Sci. Technol. 60, 649–655.
Xu, J., Liu, Y., Cui, S., Miao, X., 2006. Behavioral responses of tilapia (Oreochromis niloticus) to acute fluctuations in dissolved oxygen levels as monitored by computer vision. Aquacult. Eng. 35, 207–217.
Zhao, J., Gu, Z., Shi, M., Lu, H., Li, J., Shen, M., Ye, Z., Zhu, S., 2016. Spatial behavioral characteristics and statistics-based kinetic energy modeling in special behaviors detection of a shoal of fish in a recirculating aquaculture system. Comp. Electron. Agricult. 127, 271–280.
Zion, B., 2012. The use of computer vision technologies in aquaculture – A review. Comp. Electron. Agricult. 88, 125–132.
Zion, B., Barki, A., 2012. Ranching fish using acoustic conditioning: Has it reached a dead end? Aquaculture 344–349, 3–11.